

# Orai1 is critical for Notch-driven aggressiveness under hypoxic conditions in triple-negative breast cancers

Xiaoyu Liu<sup>a,b</sup>, Teng Wang<sup>c</sup>, Yan Wang<sup>d</sup>, Zhen Chen<sup>a</sup>, Dong Hua<sup>c</sup>, Xiaoqiang Yao<sup>b</sup>, Xin Ma<sup>a,\*</sup>, Peng Zhang<sup>a,\*</sup>

<sup>a</sup> School of Medicine, Jiangnan University, Wuxi, China

<sup>b</sup> School of Biomedical Sciences, the Chinese University of Hong Kong, Hong Kong, China

<sup>c</sup> Department of Oncology, Affiliated Hospital of Jiangnan University, Wuxi, China

<sup>d</sup> Key Laboratory of Cardiovascular Medicine and Clinical Pharmacology of Shanxi Province, Taiyuan, China

## ARTICLE INFO

### Keywords:

Orai1  
Hypoxia  
SOCE  
TNBC  
Aggressiveness

## ABSTRACT

It is believed that hypoxia stimulates triple-negative breast cancers (TNBCs) metastasis, which is associated with a poor prognosis. However, the underlying mechanism remains unclear. Here, we demonstrated that hypoxia up-regulates both the levels of Orai1 and Notch1, and the increase in Orai1 is mediated by Notch1 signaling in TNBCs. Functionally, Orai1 caused a sustained elevation of intracellular  $Ca^{2+}$  via Store-operated  $Ca^{2+}$  entry (SOCE), then activated the calcineurin-nuclear factor of activated T-cell 4 (NFAT4, also named NFATc3) in hypoxic TNBCs. Furthermore, pharmacologic inhibition or gene-silencing studies showed that the aggressiveness mediated by Orai1 during hypoxia is dependent on the Notch1/Orai1/SOCE/NFAT4 signaling. Moreover, Orai1 signaling also mediated hypoxia-induced angiogenesis in TNBCs. Thus, our results revealed a novel role of Orai1 as an inducer of aggression and angiogenesis under hypoxic conditions, and this suggests a novel mechanism of hypoxia-induced invasion. It may be worthwhile to further explore the potential of using Orai1 signaling as new target for anti-tumor therapy in TNBCs.

## 1. Introduction

Breast cancer is a leading cause of cancer-related death among women worldwide [1]. Triple-negative breast cancers (TNBCs) are characterized by lacking expression of estrogen receptor (ER), progesterone receptor (PR) and human epidermal growth factor receptor 2 (HER2), and represent 10 to 20% of breast cancer cases [2,3]. TNBCs account for early deaths of some patients because of their high rates of metastasis subtypes, and lack of effective therapeutic targets such as those for HER2 [4–6]. TNBCs are specifically heterogeneous in their molecular expression profiles through gene expression and RNA sequencing analyses [7]. Because of this heterogeneity, patients with TNBCs are limited to combination therapies consisting of surgery, chemotherapy and radiotherapy, but have worse survival rates compared with other subtypes [8]. To improve outcomes for patients with TNBCs, it will be important to identify alternative clinical strategies and develop new targeted therapies. Metastasis of TNBCs is the key reason for the failure of lasting success with surgery and for cancer recurrence. Hypoxia is a microenvironmental hallmark of most solid cancers and promotes a motile and invasive TNBCs phenotype through the

activation of hypoxia-inducible factors (HIFs). A considerable effort has been focused on exploring the mechanisms controlling hypoxia and metastasis of TNBCs, but the molecular components involved in linking hypoxia and TNBCs aggressiveness are poorly understood.

Emerging evidence suggests that Notch signaling is likely to be involved in these phenotypic changes of TNBCs [9–11]. Notch signaling plays an essential role in regulating cell fate decision, proliferation and migration during the development of many cell types [12]. Notch signaling consists of four heterodimeric transmembrane receptors (Notch1, Notch2, Notch3 and Notch4), five corresponding ligands (Jagged-1, Jagged-2, Delta-like-1, Delta-like-3 and Delta-like-4), and Notch target genes [13]. Activation of Notch signaling is thought to occur via binding of an adjacent cell's ligand at Notch receptor. After this binding, the Notch intracellular domain (NICD) is released from the plasma membrane via  $\gamma$ -secretase-mediated proteolytic cleavage, which subsequently translocates into the nucleus. NICD binds to the CSL family member RBP-JK/CBF-1, thought to mediate the expression of Notch target genes, which contain the HES and HEYL genes. CSL suppresses the transcription of Notch target genes when Notch signaling is inactive, but when Notch signaling is active, CSL acts as a

\* Corresponding authors at: School of Medicine, Jiangnan University, No. 1800 Lihu Avenue, Wuxi, China.  
E-mail addresses: [maxin@jiangnan.edu.cn](mailto:maxin@jiangnan.edu.cn) (X. Ma), [zhangpeng@jiangnan.edu.cn](mailto:zhangpeng@jiangnan.edu.cn) (P. Zhang).

<https://doi.org/10.1016/j.bbdis.2018.01.003>

Received 22 August 2017; Received in revised form 20 December 2017; Accepted 2 January 2018

Available online 05 January 2018

0925-4439/ © 2018 Elsevier B.V. All rights reserved.

transcriptional activator of same genes. Notch signaling is likely to be involved in the pathogenesis of TNBCs. High-level expression of Notch1 and Notch4 are detected by immunohistochemistry in 29 TNBC cases [14]. Notch1 and Notch3 are involved in the development of TNBCs [15,16]. Although Notch signaling plays a key oncogenic role in various malignancies, the Notch target genes that are important for the development of aggressive type are still not completely understood.

Ca<sup>2+</sup> signaling plays a critical role in regulating cell migration [17]. Previous studies showed that Ca<sup>2+</sup> influx is essential for aggression of diverse cell types, containing cancer cells [18–20]. Store-operated Ca<sup>2+</sup> entry (SOCE) is a predominant Ca<sup>2+</sup> entry pathway, in which depletion of intracellular stores stimulates Ca<sup>2+</sup> entry from extracellular milieu [21]. The literatures showed that Orai1 and STIM1 are responsible for SOCE, in which STIM1 serves as a Ca<sup>2+</sup> sensor in sarco/endoplasmic reticulum whereas Orai1 is an essential pore-forming component for Ca<sup>2+</sup> permeation.

Decreased Ca<sup>2+</sup> in sarco/endoplasmic reticulum induces STIM1 oligomerization and relocation to the regions immediately underneath the plasma membrane, where it binds to Orai1 to cause Ca<sup>2+</sup> influx [22,23]. Interestingly, Orai1 is reported to play essential roles in promoting tumor cell migration. Elevated Orai1 expression promotes human gastric cancer cell migration and invasion [24]. Yang et al. reported that Orai1 is critical for breast tumor cell migration and metastasis in vivo and in vitro [25]. However, the mechanism by which Orai1 induces tumor cell aggression under hypoxic conditions remains unclear.

Given these findings, we hypothesized that Notch pathway and Orai1 regulate TNBCs aggression under hypoxic conditions. Therefore, we set out to test this hypothesis by investigating the relationship between Notch signaling and Orai1 in hypoxic TNBCs. We found that inhibition of the Notch pathway in TNBCs blocks the hypoxia-induced up-regulation of Orai1. Induction of Orai1 promotes the aggressive type by increasing a SOCE regulated elevation of intracellular Ca<sup>2+</sup> level, which then activates NFAT4, and this is critical for TNBCs invasion and angiogenesis. Collectively, these data revealed that hypoxia maintains aggression in TNBCs by regulating Notch signaling and Orai1, suggesting that this regulation is an important component of how hypoxia controls the aggression and angiogenesis in TNBCs.

## 2. Materials and methods

### 2.1. Ethics statement and patients

The study using clinical samples was approved by the Review Board of the Affiliated Hospital of Jiangnan University. The human triple-negative breast cancer samples (n = 69) were from Affiliated Hospital of Jiangnan University. Informed consent was requested as anonymous specimens and was given by all human participants in this study. Patients were recruited between 2010 and 2013.

### 2.2. Drugs and antibodies

SKF96365 (1147), FK506 (3631) and thapsigargin (1138) from Tocris Bioscience; DAPT (S2215) from Selleckchem; Alexa Fluor 568 Donkey anti-Rabbit IgG (H + L) Antibody and Alexa Fluor 488 Donkey Anti-Mouse IgG (H + L) Antibody from Life Technologies Corp; anti-Orai1 antibody (O8264) from Sigma; anti-NFAT4 antibody (sc-8405) and anti-ATCB antibody (sc-47778) from Santa Cruz Biotechnology; anti-Notch1 antibody (#3608), anti-Cleaved Notch1 antibody (#4147) and anti-Jagged1 antibody (#2620) from Cell Signaling Technology; anti-HIF1 $\alpha$  antibody (610958) from BD Biosciences; anti-TATA binding protein antibody (TBP; ab51841) from Abcam.

### 2.3. Cell culture and exposure to hypoxia

MDA-MB 231, BT549 and HMEC-1 cells were from the American

Type Culture Collection. MDA-MB 231 and BT549 cells were cultured in RPMI 1640 (Gibco) supplemented with 10% FBS (Gibco), 100  $\mu$ g/mL penicillin and 100 U/mL streptomycin (Gibco). HMEC-1 cells were cultured in endothelial cell growth medium (EGM) supplemented with bovine brain extract (Lonza). To establish hypoxic conditions, the cells were cultured at 1% oxygen, 94% N<sub>2</sub> and 5% CO<sub>2</sub> at 37 °C using humidified multigas incubator [26]. The normoxic control cells were incubated at 37 °C with 5% CO<sub>2</sub> in a humidified incubator.

### 2.4. Analysis of mRNA expression by real-time PCR

To determine the mRNA expression, real-time PCR analysis was performed. Total RNA was isolated from cells using TRIzol Reagent (Invitrogen), and treated with DNase I (Invitrogen). cDNA was synthesized from 1  $\mu$ g total RNA, using random primers with a High Capacity cDNA Reverse Transcription Kit (Applied Biosystems). Gene expression was normalized against ACTB. The primer sequences used were: ACTB forward 5'-CACCATTGGCAATGAGCGGTTTC-3', reverse

5'-AGGTCITTTGCGGATGTCCACGT-3'; HIF1 $\alpha$  forward 5'-AGCTTGC TCATCAGTTGCCA-3', reverse 5'-CCAGAAGTTTCTCACACGC-3'; Jagged1 forward 5'-TGCTACAACCGTGCCAGTGACT-3', reverse 5'-TCA GGTGTGTCGTTGGAAGCCA-3'; Notch1 forward 5'-CCCAGGAATCTGA GATGGAA-3'; reverse 5'-CCACAGCAAAGTCTGACAT-3'; HEYL forward 5'-TGGAGAAAGCCGAGGTCTTGCA-3', reverse 5'-ACCTGATGAC CTCAGTGAGGCA-3'; HES1 forward 5'- GTGGGTCCTAACGCAGT GTC-3'; reverse 5'- GTCAGAAGAGAGAGGTGGGCTA -3'; HES5 forward 5'- ATGCTCAGTCCCAAGGAGAA -3', reverse 5'- CTCCAGCAGAGTTT CAGC-3'; Orai1 forward 5'-GCCCTTCGGCCTGATCTTTAT-3'; reverse 5'- TGGAAGTTCGGTCAGTCTTAT-3'; Real-time PCR was performed with 7500 Fast Real-time PCR system (Applied Biosystems), using Power SYBR Green PCR Master Mix (Applied Biosystems).

### 2.5. siRNA and shRNA knockdown analyses

For knockdown of Notch1 and NFAT4 transcripts, MDA-MB 231 and BT549 cells were transiently transfected with gene-specific or scrambled small interfering RNA (siRNA) using DharmaFECT 1 Transfection Reagent (GE Healthcare) following the standard procedure recommended by the manufacturer. The human pool siRNAs was obtained from Santa Cruz. In brief, cells were transfected in RPMI 1640 medium with 100 nM of each siRNA duplexes using DharmaFECT transfection reagent according to the manufacturer's protocol [27].

Two short hairpin RNA (shRNA) constructs against human Orai1 were generated using the pSUPER.puro vector according to the manufacturer's instructions (OligoEngine). The sequences used were 5'-CGT GCACAATCTCAACTCG-3' (in coding region) and 5'-CCAGCATTGAGT GTGTACA-3' (in 3'-UTR) as described elsewhere [25,28]. Transfection with shRNA plasmid was carried out using the Lipofectamine 2000 Transfection Reagent (Invitrogen) according to the manufacturer's instructions.

### 2.6. Western blot analysis

Cells were lysed in a detergent extraction buffer containing 1% (vol/vol) Nonidet P-40, 150 mmol/L NaCl, and 20 mmol/L Tris-HCl, pH 8.0, with protease inhibitor cocktail tablets for 30 min on ice and centrifuged for 15 min at 4 °C. The nucleic fractions were prepared using Nuclear and Cytoplasmic Protein Extraction kit (Beyotime Biotech). Cells were mixed with the cytoplasmic extraction buffer on ice for 15 min. Suspension was shaken vigorously and centrifuged for 5 min at 4 °C. The supernatant was discarded and the pellet was re-suspended in nuclear extraction buffer on ice for 30 min. The resulting supernatant was used as nucleic fractions following centrifuge for 10 min. Protein concentrations were then measured using a Bio-Rad protein assay kit (Hercules, CA). Proteins were separated on an 8–12% gel using sodium dodecyl sulfate polyacrylamide gel electrophoresis. For immunoblots,

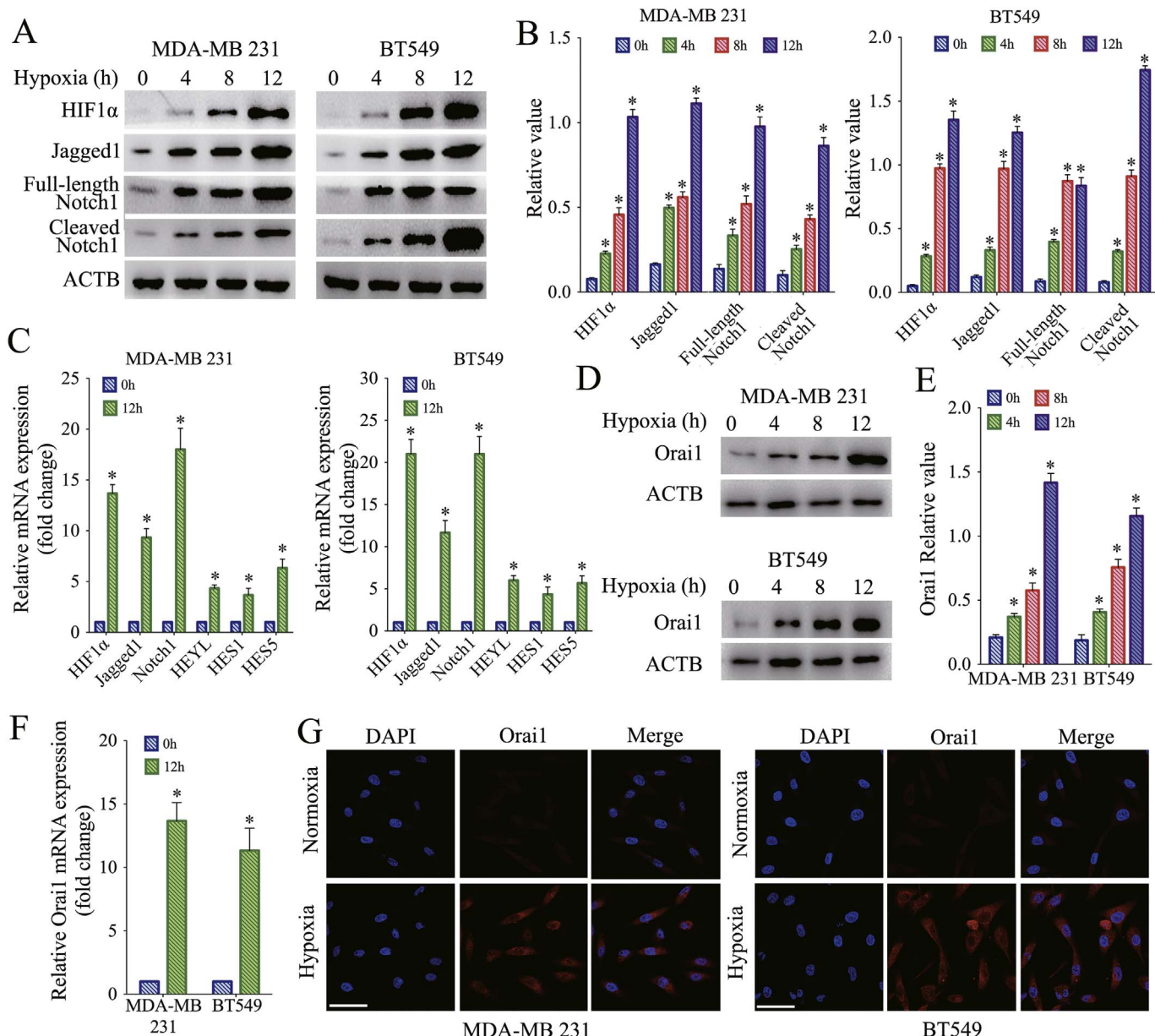


**Fig. 1. Hypoxia promotes Notch signaling and Orai1 expression in TNBCs.**

**A and B,** Representative images and summary data from western blotting showing the time course of HIF1 $\alpha$ , Jagged1, Full-length Notch1, Cleaved Notch1 and ACTB expression in hypoxic MDA-MB 231 and BT549 cells. **C,** Real-time PCR for HIF1 $\alpha$ , Jagged1, Notch1, HEYL, HES1 and HES5 mRNA in hypoxic TNBCs. **D and E,** Representative images and summary data from western blotting showing the time course of Orai1 in hypoxic TNBCs. **F,** Summary data from real-time PCR for Orai1 mRNA in hypoxic TNBCs. **G,** Representative images from immunofluorescence of Orai1 in hypoxic TNBCs. Scale bars, 50  $\mu$ m. Values are means  $\pm$  SEM of three to six experiments. \*,  $p < 0.05$ , compared to 0 h (normoxia).

the polyvinylidene difluoride membrane carrying the transferred proteins was incubated at 4  $^{\circ}$ C overnight with designated primary antibodies diluted in TBST buffer pH 7.5, containing 50 mM Tris, 150 mM NaCl, 0.1% Tween20, and 5% BSA. Immunodetection was accomplished using a horseradish peroxidase-conjugated secondary antibody and an enhanced chemiluminescence detection system (GE Healthcare). Densitometry analyses were performed using ImageJ software (NIH), and ACTB or TBP control was used to confirm equal sample loading and normalization of the data [29].

### 2.7. Immunofluorescence analysis

Immunofluorescence staining was performed as previously described [30]. Briefly, cultured cells were fixed with 4% paraformaldehyde (PFA, Sigma-Aldrich) for 15 min then blocked with 10% BSA with 0.1% Triton X-100 (Bio-Rad) in PBS for 30 min at room temperature.

Samples were incubated with primary antibodies overnight at 4  $^{\circ}$ C followed by the appropriate secondary fluorescently labeled antibodies (Invitrogen Molecular Probes) for 1 h at room temperature. Nuclei were counterstained with DAPI (4',6-diamidino-2-phenylindole, Life Technologies). The samples were visualized under FV1000 laser scanning confocal microscope.

### 2.8. $[Ca^{2+}]_i$ measurement

$[Ca^{2+}]_i$  measurements were performed as previously described [31]. Briefly, cells were loaded with Fura-2/AM (Invitrogen) in normal Tyrode's solution that contained in mM: 140 NaCl, 5.4 KCl, 1 MgCl<sub>2</sub>, 2 CaCl<sub>2</sub>, 5.5 glucose, and 5 HEPES, pH 7.4. The Ca<sup>2+</sup>-bound and -unbound Fura-2 fluorescence signals were measured using dual excitation wavelengths at 340 and 380 nm using an Olympus fluorescence imaging system. Fura-2 ratio change was then converted to  $[Ca^{2+}]_i$ . The

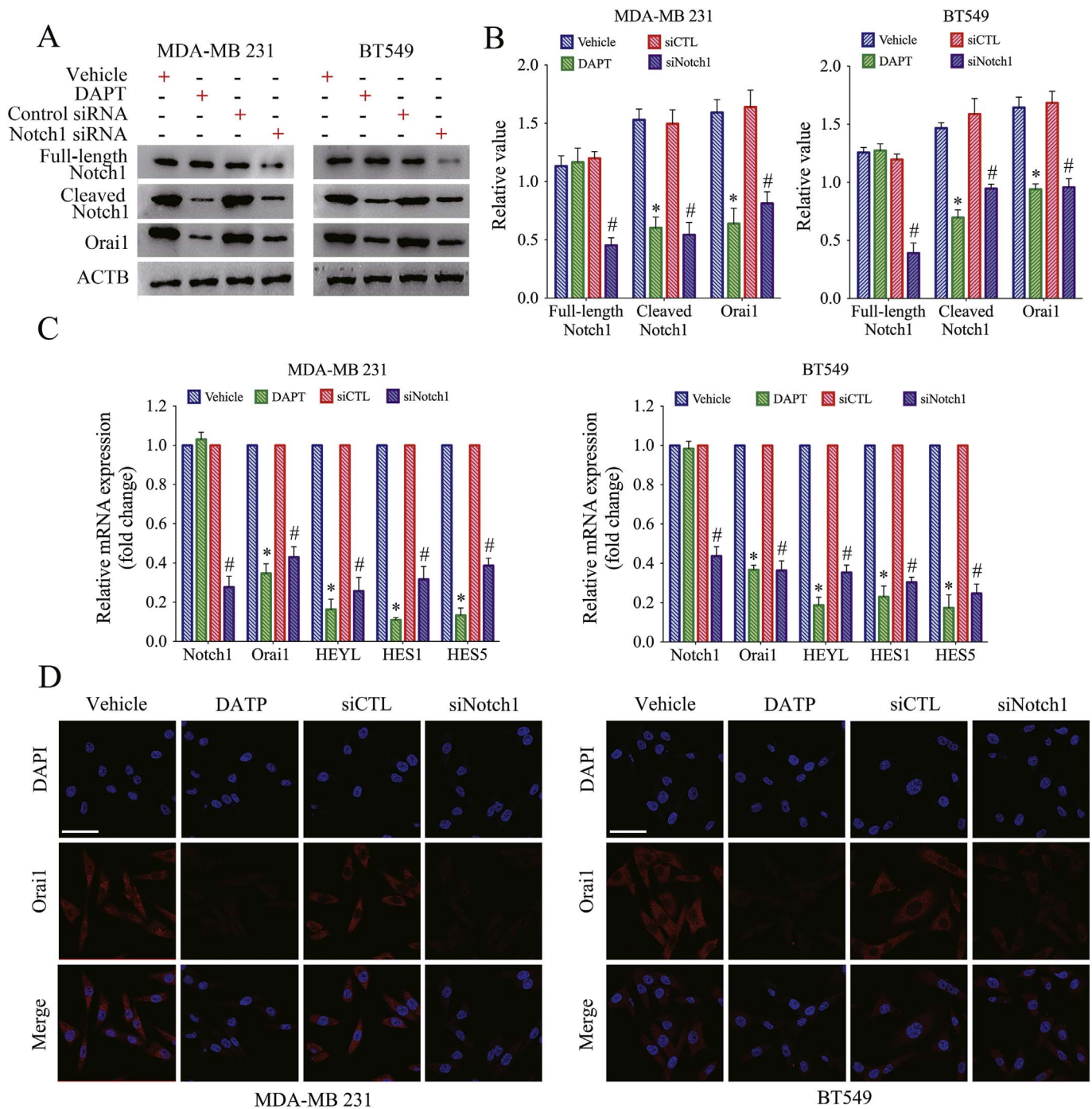


**Fig. 2. Hypoxia induces Notch signaling-dependent Orai1 expression in TNBCs.**

**A and B,** Representative images and summary data from Full-length Notch1, Cleaved Notch1, Orai1 and ACTB protein levels in MDA-MB 231 and BT549 cells that were pretreated with DAPT (75  $\mu$ M) for 2 h or transfected with specific siRNA before exposure to hypoxia 12 h. **C,** Summary data from real-time PCR for Notch1, Orai1, HEYL, HES1 and HES5 mRNA in TNBC pretreated as in **A.** **D,** Representative images from immunofluorescence of Orai1 in hypoxic TNBCs as in **A.** Scale bars, 50  $\mu$ m. Values are means  $\pm$  SEM of three to seven experiments. \*,  $p < 0.05$ , compared to Vehicle, #,  $p < 0.05$ , compared to siCTL.

conversion was based on a standard curve that was constructed using commercially available  $Ca^{2+}$  standard solutions of different concentrations. The fluorescence in an area without cells was taken as background and subtracted.

### 2.9. SOCE and basal $Ca^{2+}$ influx measurement

SOCE measurement was performed as described previously [28]. Briefly, cells were loaded with Fura-2/AM in normal Tyrode's solution. For store depletion, cells were pretreated with 4  $\mu$ M thapsigargin for

15 min in  $Ca^{2+}$ -free Tyrode's solution, which contained in mM: 140 NaCl, 5.4 KCl, 1  $MgCl_2$ , 5.5 glucose, 0.2 ethylene glycol tetraacetic acid (EGTA), and 5 HEPES, pH 7.4.  $Ca^{2+}$  influx was initiated by the addition of 2 mM  $Ca^{2+}$  to the bath. Basal  $Ca^{2+}$  influx was measured by starting the cells in the  $Ca^{2+}$ -free Tyrode's solution without thapsigargin and then adding 2 mM  $Ca^{2+}$  to the solution. Fura-2 fluorescence signals were measured using dual excitation wavelengths at 340 and 380 nm using an Olympus fluorescence imaging system. Change in  $Ca^{2+}$  was displayed as change in Fura-2 ratio. 10 to 20 cells were analyzed in each experiment.

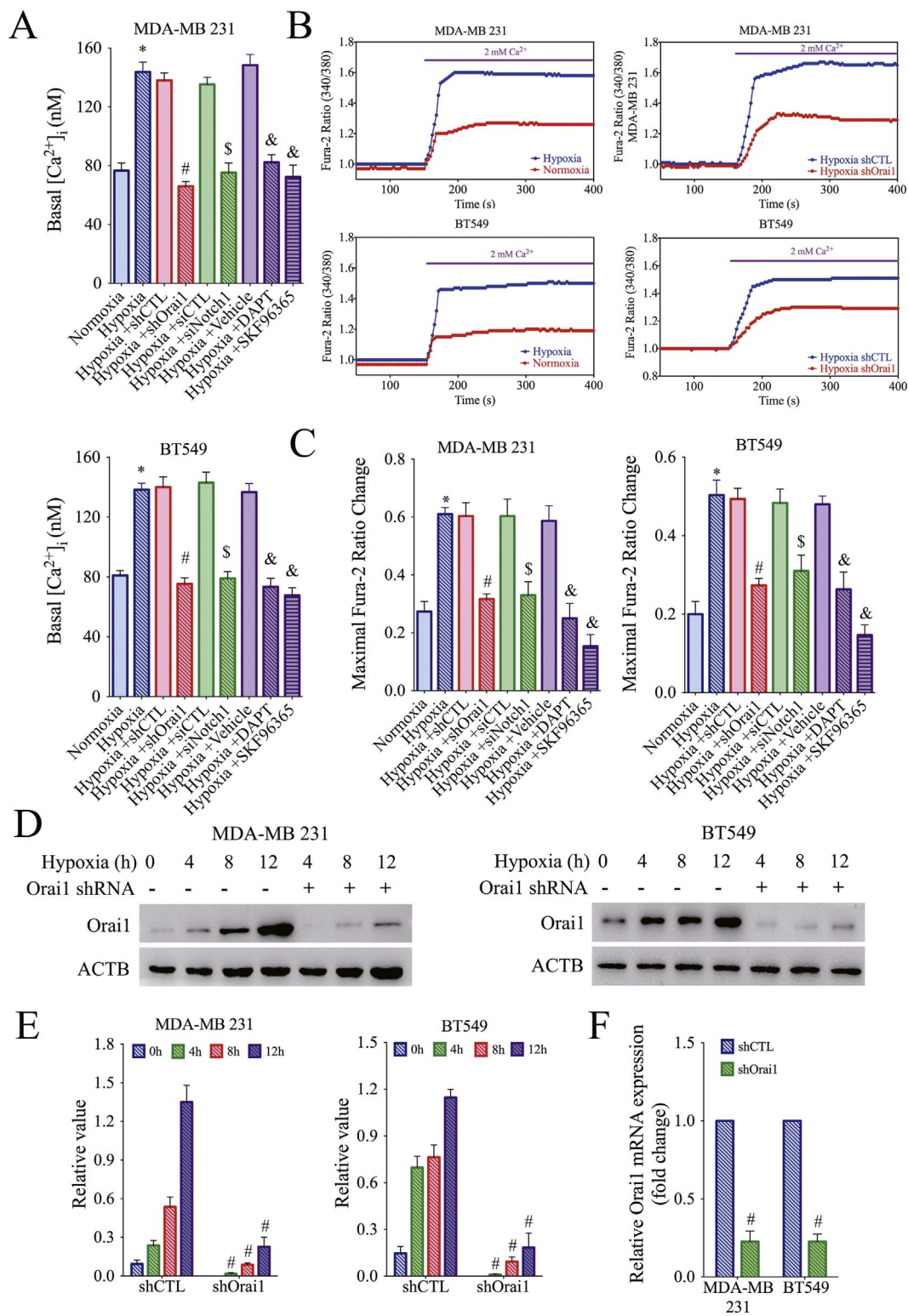


**Fig. 3.** Orai1 augments SOCE in TNBCs exposed to hypoxia.

A, Summary data from basal  $[Ca^{2+}]_i$  in MDA-MB 231 and BT549 cells that were pretreated with DAPT (75  $\mu$ M) for 2 h, SKF96365 (10  $\mu$ M) for 2 h or transfected with specific siRNA/shRNA before exposure to hypoxia 12 h. B and C, Representative images and summary data from SOCE measurement in MDA-MB 231 and BT549 cells that were pretreated as in A. D and E, Representative images and summary data from western blotting showing the time course of Orai1 and ACTB in TNBCs cultures that were transfected with Orai1 shRNA. F, Summary data from real-time PCR for Orai1 mRNA in TNBCs transfected with Orai1 shRNA before exposure to hypoxia 12 h. Values are means  $\pm$  SEM of three to six experiments. \*,  $p < 0.05$ , compared to normoxia, #,  $p < 0.05$ , compared to shCTL, \$,  $p < 0.05$ , compared to siCTL, &,  $p < 0.05$ , compared to Vehicle.

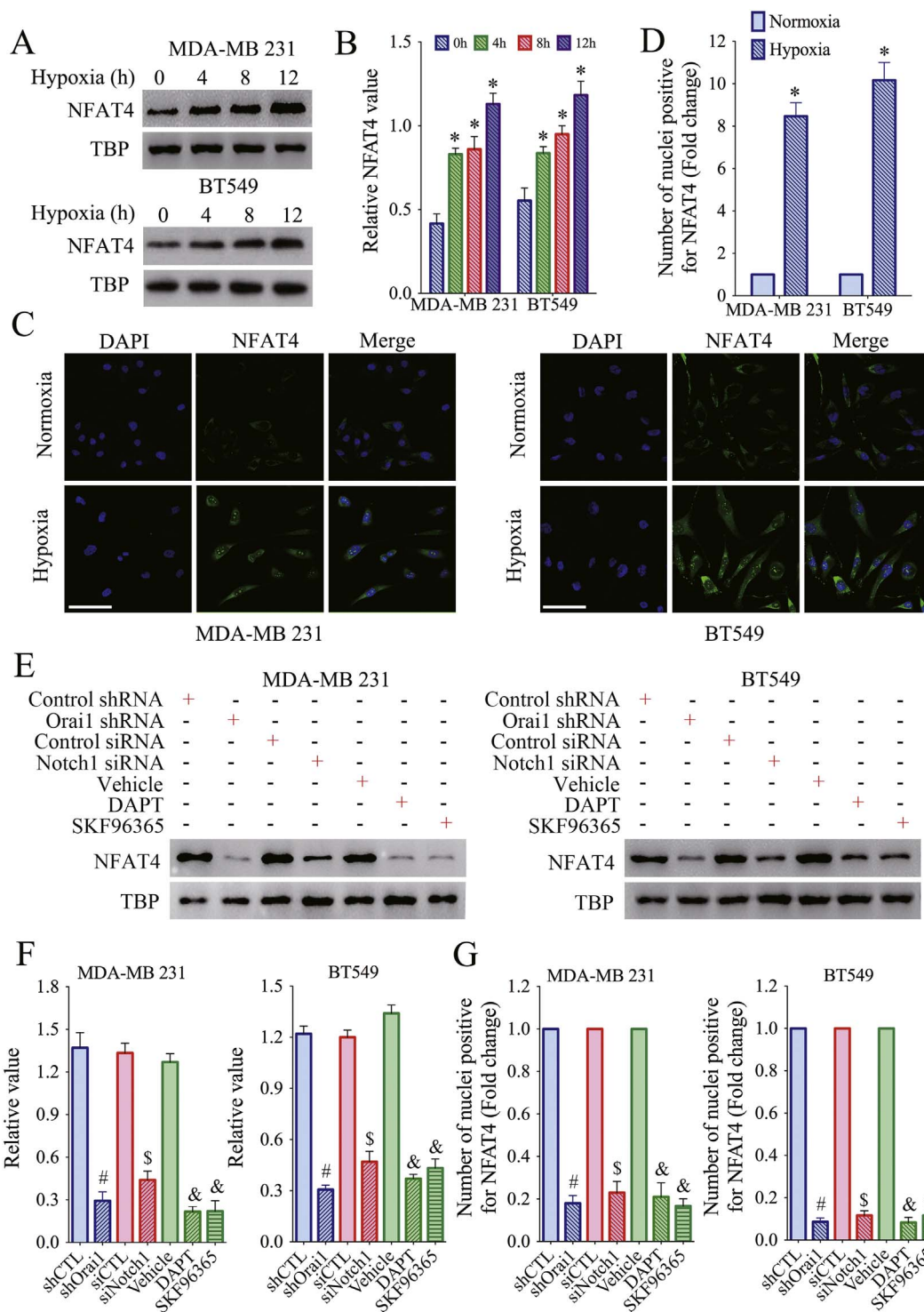


**Fig. 4.** Orai1-regulated SOCE mediates NFAT4 activation in TNBCs exposed to hypoxia.

**A and B,** Representative images and summary data from western blotting showing the time course of NFAT4 and TBP expression in hypoxic MDA-MB 231 and BT549 cells. **C and D,** Representative images and summary data from immunofluorescence for nuclear translocation of NFAT4 in MDA-MB 231 and BT549 cells exposure to hypoxia or normoxia. Scale bars, 50  $\mu$ m. **E and F,** Representative images and summary data from western blotting showing the time course of NFAT4 and TBP expression in hypoxic MDA-MB 231 and BT549 cells that were pretreated with DAPT (75  $\mu$ M) for 2 h, SKF96365 (10  $\mu$ M) for 2 h or transfected with specific siRNA/shRNA before exposure to hypoxia 12 h. **G,** Summary data from immunofluorescence for nuclear translocation of NFAT4 in MDA-MB 231 and BT549 cells that were pretreated as in E. Values are means  $\pm$  SEM of three to six experiments. \*,  $p < 0.05$ , compared to hypoxia 0 h or normoxia, #,  $p < 0.05$ , compared to shCTL, \$,  $p < 0.05$ , compared to siCTL, &,  $p < 0.05$ , compared to Vehicle.

### 2.10. Wound healing assay

The wound healing assay used was a monolayer denudation assay as described previously [32]. Briefly, cells cultured in 12-well plates as confluent monolayers were mechanically scratched using a 200  $\mu$ L

pipette tip to create the wound. Cells were washed with PBS to remove the detached cells and then cultured to allow migration. Photographs were taken and the percent of wound closure was calculated.

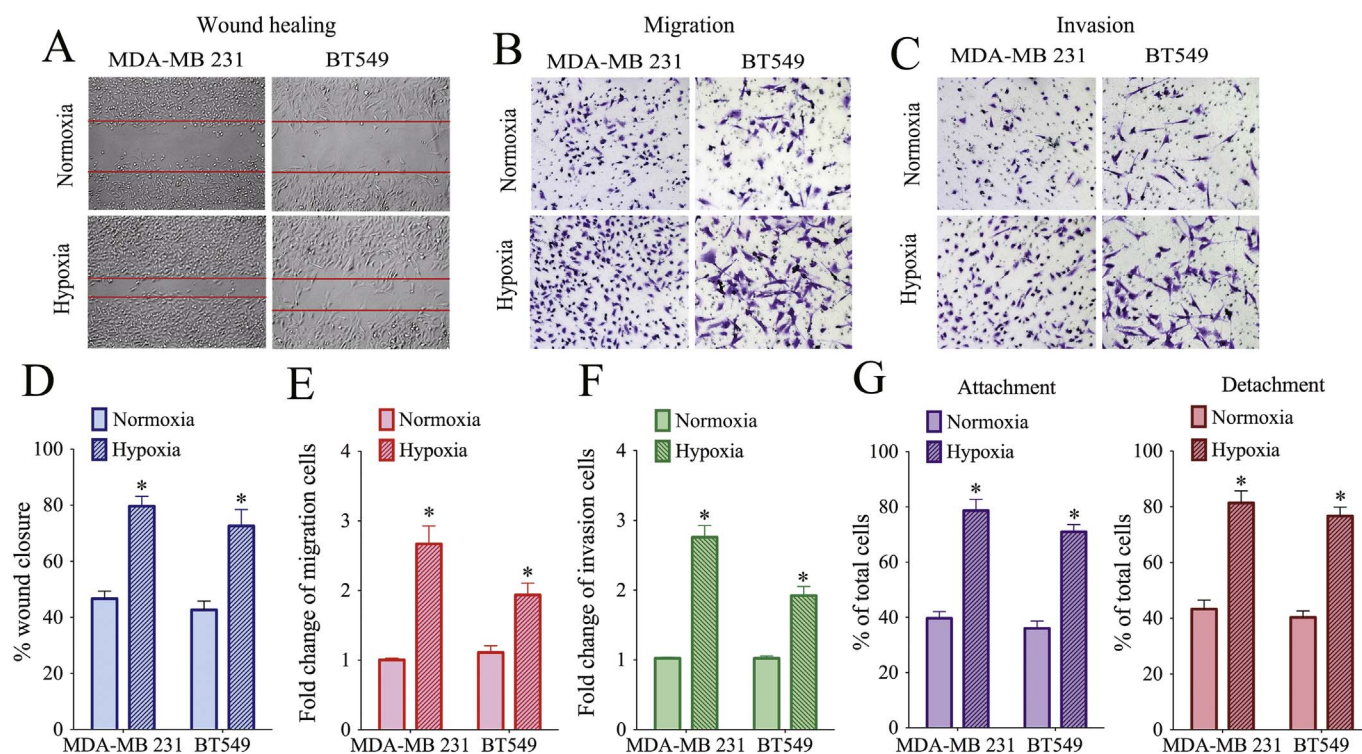


**Fig. 5. Hypoxia increases cell migration and invasion in TNBCs.**

A, Motility of MDA-MB 231 and BT549 cells exposure to hypoxia 16 h or normoxia was examined by wound healing assay. B, Migration capacity of TNBCs exposure to hypoxia 16 h or normoxia was examined by transwell assay. C, Invasion capacity of TNBCs exposure to hypoxia 16 h or normoxia was examined by matrigel invasion assay. D to F, Summary data of wound healing assay, migration assay and invasion assay described as in A to C. G, Summary data form attachment and detachment assay in hypoxic TNBCs. Values are means  $\pm$  SEM of three to six experiments. \*,  $p < 0.05$ , compared to normoxia.

### 2.11. Transwell migration assay

Cell migration assays were performed in the absence of a Matrigel layer and used transwell chamber (Corning) [33]. Transwell inserts were suspended on the individual wells of 24-well plates. Briefly, cells were harvested, washed, resuspended and then seeded into the upper chamber in serum-free medium at a density of  $2 \times 10^5$  cells/well. The medium containing 10% FBS was placed in the lower chamber and the cells were further incubated for 24 h, cells in the upper chamber were removed with a cotton swab, and the rest of the membrane had invaded the cells. Cells migrated through the membrane were fixed with 4% paraformaldehyde and stained with crystal violet. The number of migrated cells was counted in 5 randomly selected microscopic fields and photographed.

### 2.12. Invasion assay

Cell invasion was determined with Matrigel matrix (BD Biosciences) coated on the upper surface of the transwell chamber (Corning). Cells were seeded, fixed, stained and counted as described in transwell migration assay.

### 2.13. Cell attachment and detachment assays

Cell attachment and detachment assay was done as described previously [34]. For cell attachment assay, the cells were seeded in 24-well plates at  $5 \times 10^4$  per well. After 1-hour incubation, unattached cells were removed, and the attached cells were counted after trypsinization. The data were presented as a percentage of the cells attached to the plate compared with total cells. For cell detachment assay, the cells were seeded in 24-well plates at  $5 \times 10^4$  per well. After 24-hour incubation, the medium was removed and the cells were incubated with 0.05% trypsin for 3 min to detach the cells from the culture plates. The

medium containing 10% fetal bovine serum was added into the cells to inactivate the trypsin and the detached cells were collected into tubes. The remaining cells were incubated with 0.25% trypsin to detach all the cells and collected into fresh tubes. The cells were counted and the data were presented as a percentage of the detached cells to total cells.

### 2.14. Endothelial cell tube formation assay

The tube formation assay was done as previously described [29]. Briefly, HMEC-1 cells were seeded in the matrigel-coated culture plates and suspended in conditioned medium collected from MDA-MB 231 and BT549 cells with different treatments.

### 2.15. Immunohistochemistry staining

Tissue slides were deparaffinized with xylene and rehydrated through a graded alcohol series. The endogenous peroxidase activity was blocked by incubation in a 3% (vol/vol) hydrogen peroxide solution for 10 min. Antigen retrieval was carried out by immersing the slides in 10 mM sodium citrate buffer (pH 6.0) and maintaining them at a subboiling temperature for 10 min. The slides were incubated with the primary antibody in 10% (wt/vol) BSA and 0.4% sodium azide in PBS at 4 °C in a humidified chamber. Subsequently, the sections were incubated with the GTVision III Detection System/Mo&Rb Kit (Gene Tech Company Limited). All staining was assessed by pathologists blinded to the origination of the samples and subject outcome. The widely accepted German semiquantitative scoring system for considering the staining intensity and area extent was used. Each specimen was assigned a score according to the staining (0, no staining; 1, weak staining; 2, moderate staining; 3, strong staining) and the extent of stained cells (0, 0%; 1, 1–24%; 2, 25–49%; 3, 50–74%; 4, 75–100%). The final immunoreactive score was determined by multiplying the intensity score with the extent of score of stained cells, ranging from 0

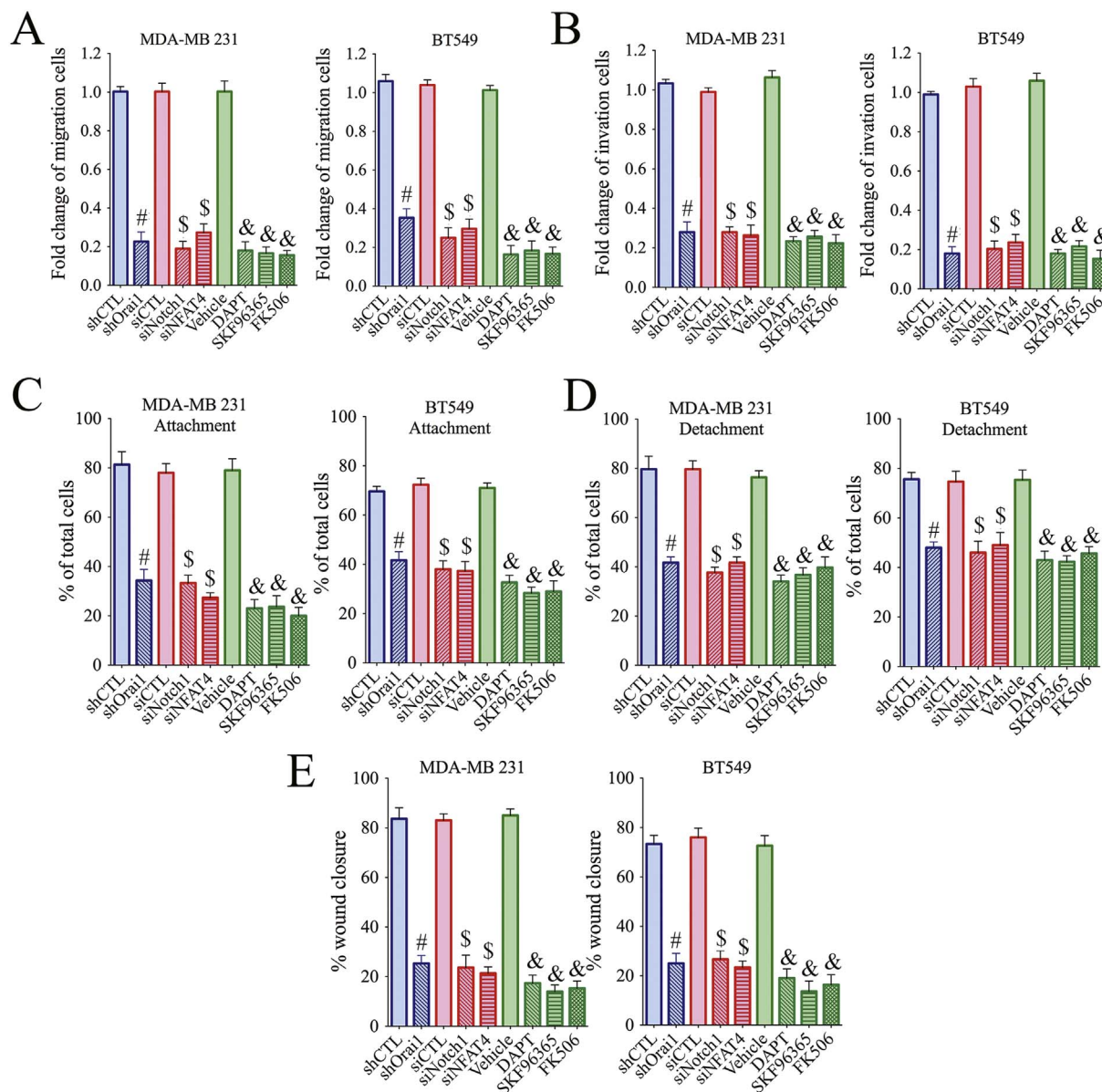


**Fig. 6.** Orai1 regulates hypoxia-induced cell migration and invasion in TNBCs.

**A**, Summary data from migration assay showing the effects of specific siRNA/shRNA, DAPT (75  $\mu$ M), SKF96365 (10  $\mu$ M) or FK506 (1  $\mu$ M) in hypoxic TNBCs. **B**, Summary data from invasion assay showing the effects of different treatments described as in **A**. **C**, Summary data from attachment assay in TNBCs described as in **A**. **C**, Summary data from detachment assay in TNBCs described as in **A**. **E**, Summary data of wound healing assay in TNBCs described as in **A**. Values are means  $\pm$  SEM of three to six experiments. #,  $p < 0.05$ , compared to shCTL, \$,  $p < 0.05$ , compared to siCTL, &,  $p < 0.05$ , compared to Vehicle.

(the minimum score) to 12 (the maximum score).

### 2.16. Statistical analyses

Data were expressed as mean  $\pm$  SEM of at least 3 independent experiments. Statistical analysis was performed using the 2-tailed Student's *t*-test or one-way ANOVA. All analyses were performed using GraphPad Prism version 5. The difference was considered significant if  $p < 0.05$ .

## 3. Results

### 3.1. Hypoxia promotes Notch signaling and Orai1 expression in TNBCs

Intratumoral hypoxia contributes to a motile and invasive type through the activation of HIFs and independently predicts poor outcome to chemotherapy and radiation in various solid cancers including

breast cancers. It is reported that Notch1 and Jagged-1 exist in human TNBC cell lines and clinical TNBC specimens. Because Notch signaling regulates cell fate decision and migration during development of numerous cancer cell types, we investigated Notch signaling in TNBCs under hypoxia. For this purpose, we exposed the human TNBC cell line MDA-MB 231 and BT549 to 1%  $O_2$  to mimic hypoxic condition and detected the expression of full-length Notch1 and its ligand Jagged-1 by western blotting. Cleaved-Notch1 was also detected, which represents the activated form of Notch1. The increased protein expression of full-length Notch1, cleaved-Notch1 and Jagged-1 was time dependent in the case of MDA-MB 231 and BT549 exposed to hypoxia (Fig. 1A and B). Transcriptional alterations of Notch1 and Jagged-1 were also determined by quantitative real-time PCR and results revealed that Notch1 and Jagged-1 mRNA expressions were increased under hypoxic treatment (Fig. 1C). As control for the hypoxic effect, HIF1 $\alpha$  was significantly enhanced in both cell lines (Fig. 1A to C). To further confirm the increase in Notch activity, the mRNA expression of the Notch target

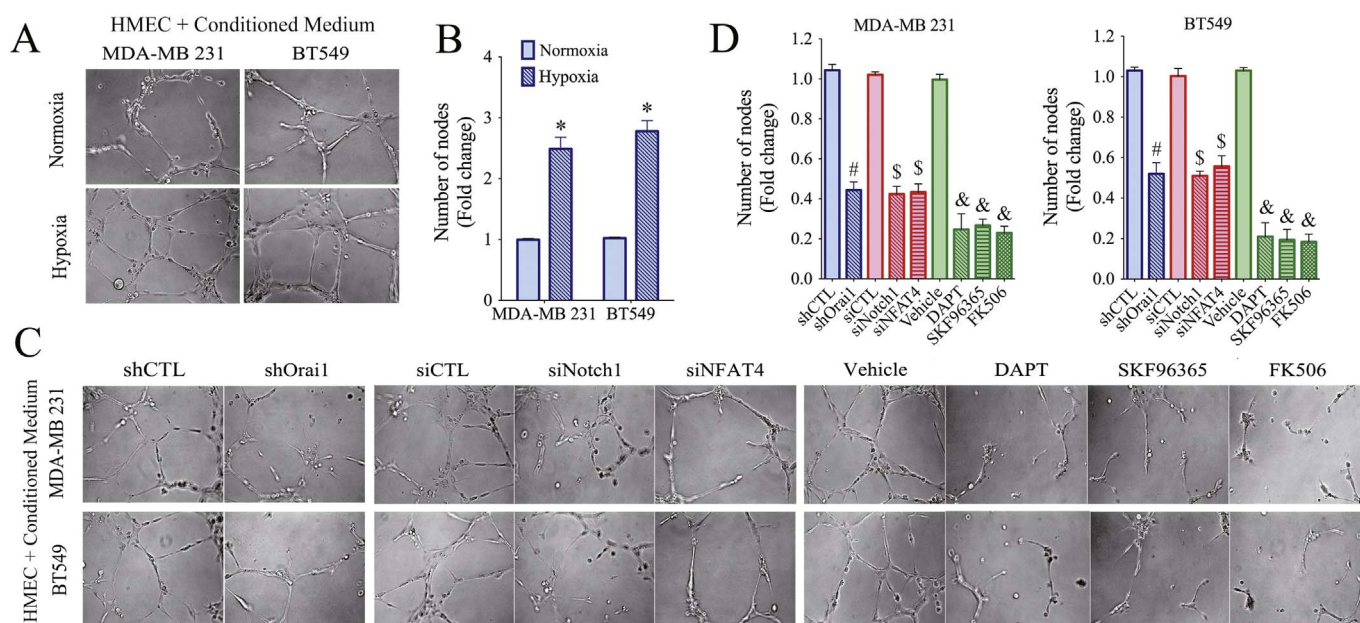


**Fig. 7. Orai1 supports hypoxia-induced angiogenesis in TNBCs.**

**A and B**, Representative images and summary data from tube formation showing the degree of angiogenic induction in HMECs grown in conditioned medium harvested from MDA-MB 231 or BT549 cells under hypoxia or normoxia. **C and D**, Representative images and summary data from tube formation showing the degree of angiogenic induction in HMECs grown in conditioned medium harvested from MDA-MB 231 or BT549 cells with specific siRNA/shRNA, DAPT (75  $\mu$ M), SKF96365 (10  $\mu$ M) or FK506 (1  $\mu$ M) under hypoxia conditions. Values are means  $\pm$  SEM of three to five experiments. #,  $p < 0.05$ , compared to shCTL, \$,  $p < 0.05$ , compared to siCTL, &,  $p < 0.05$ , compared to Vehicle.

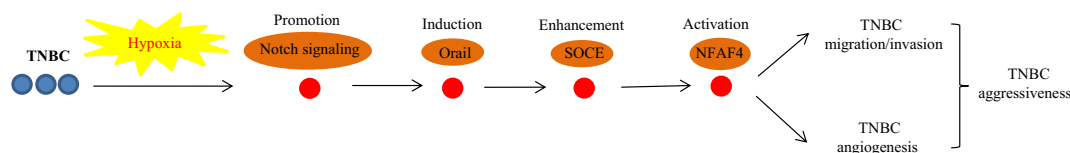


**Fig. 8. Model of the roles of Orai1 in TNBC aggressiveness under hypoxia.**

Hypoxia promotes Notch signaling and then induces Orai1 expression. Up-regulated Orai1 expression increases the basal  $[Ca^{2+}]_i$  via SOCE and then activates NFAT4. Activation of NFAT4 supports TNBC invasion and angiogenesis under hypoxic conditions. Arrows represent promotion events.

genes HEYL, HES1 and HES5 were observed. We found that Notch target genes were specifically elevated (Fig. 1C), suggesting that the activation of Notch signaling is sustained in hypoxic TNBC cells via a potential mechanism of ligand-dependent stimulation of the Notch receptor. Orai1 is recently reported to be involved in tumor cell migration and metastasis. To explore the expression of Orai1 in TNBCs, we quantified Orai1 transcripts and proteins in hypoxia-treated MDA-MB 231 and BT549 cells. Orai1 mRNA and protein level were significantly elevated under hypoxia compared with normoxia (Fig. 1D to F). Immunofluorescence staining also confirmed that the protein level of Orai1 was significantly elevated in MDA-MB 231 and BT549 cells after the hypoxic switch (Fig. 1G). These experiments showed that hypoxia activates Notch signaling and up-regulates Orai1 expression in TNBCs.

### 3.2. Hypoxia induces Notch signaling-dependent Orai1 expression in TNBCs

To determine whether hypoxia-induced Orai1 expression requires the activation of Notch signaling in TNBCs, we investigated the impact of pharmacologically inhibiting on the progression of Notch to cleaved-Notch using DAPT, a small molecule Notch signaling inhibitor. Gene silencing of Notch1 was also used. Notch1 expression was used to assess the level of inhibition of Notch signaling. We found that the protein levels of full-length Notch1 and cleaved-Notch1 were significantly decreased in MDA-MB 231 and BT549 cells after silencing of Notch1 (Fig. 2A and B). DAPT markedly decreased the level of cleaved-Notch1 protein expression but not full-length Notch1 (Fig. 2A and B). In addition, DAPT and Notch1 silencing decreased the Notch target genes

HEYL, HES1 and HES5 mRNA expression (Fig. 2C). These results showed that pharmacological inhibition or gene silencing of Notch1 effectively suppresses the induction of Notch signaling in response to hypoxia. To determine whether Notch signaling is crucial for Orai1 expression exposed to hypoxia, we examined the transcriptional and translational alterations of Orai1 in TNBCs exposed to hypoxia. The results showed that DAPT markedly decreases hypoxia-induced Orai1 expression (Fig. 2A to D). Next, down-regulated of Notch1 strongly inhibited hypoxia-induced Orai1 expression (Fig. 2A to D). Collectively, these data suggested that Notch signaling up-regulates Orai1 expression in response to hypoxia.

### 3.3. Orai1 augments SOCE in TNBCs exposed to hypoxia

To address whether the hypoxia-induced Orai1 expression contributes to a sustained enhancement of cytosolic  $Ca^{2+}$  concentration ( $[Ca^{2+}]_i$ ) in TNBCs, we investigated the basal  $[Ca^{2+}]_i$  by using Fura-2. After exposing to hypoxia for 12 h, basal  $[Ca^{2+}]_i$  were remarkably increased in MDA-MB 231 and BT549 cells (Fig. 3A). DAPT treatment or down-regulation of Notch1 decreased basal  $[Ca^{2+}]_i$  in MDA-MB 231 and BT549 cells exposed to hypoxia (Fig. 3A). To measure the SOCE, MDA-MB 231 or BT549 cells in  $Ca^{2+}$  free solution were treated with 4  $\mu$ M thapsigargin (TG) for 15 min to deplete intracellular  $Ca^{2+}$  stores, followed by adding 2 mM  $Ca^{2+}$  to the bath. A markedly increased SOCE were observed in MDA-MB 231 and BT549 cells under hypoxia compared with normoxia (Fig. 3B and C). Next, to verify that Orai1 was responsible for the up-regulated basal  $[Ca^{2+}]_i$  and TG-induced SOCE in

hypoxic TNBCs, we selectively down-regulation Orai1 expression using two Orai1-specific shRNAs. The knockdown effects of two Orai1-specific shRNAs in TNBCs were verified by quantitative real-time PCR and western blotting (Fig. 3D to F). Silencing of Orai1 suppressed the hypoxia-induced elevation of  $[Ca^{2+}]_i$  and TG-induced SOCE in hypoxic MDA-MB 231 and BT549 cells (Fig. 3A to C). We also found that DAPT treatment or down-regulation of Notch1 reduced TG-induced SOCE (Fig. 3B and C). In addition, SKF96365, used as a pharmacological inhibitor of SOCE, resulted in reduced basal  $[Ca^{2+}]_i$  and TG-induced SOCE in hypoxic TNBCs (Fig. 3A to C). Moreover, we also measured basal  $Ca^{2+}$  influx by starting the cells in the  $Ca^{2+}$ -free solution without thapsigargin and then adding 2 mM  $Ca^{2+}$  to the solution. The results showed that down-regulation of Orai1 suppressed the increase in hypoxia-induced basal  $Ca^{2+}$  influx (Supplementary Fig. 1). These results indicated that Orai1 is mainly responsible for the enhanced basal  $[Ca^{2+}]_i$  and TG-induced SOCE in hypoxic TNBCs.

### 3.4. Orai1-regulated SOCE mediates NFAT4 activation in TNBCs exposed to hypoxia

It is reported that Orai1-regulated SOCE activates downstream targets including NFAT signaling, which plays an important role in promoting tumor processing [35,36]. Thus, we investigated whether Orai1-regulated SOCE evaluates NFAT4 activation in hypoxic TNBCs. The results showed that NFAT4 expression was considerably up-regulated in the nucleus in hypoxic MDA-MB 231 and BT549 cells (Fig. 4A and B). Notably, nuclear localization of NFAT4 was also measured by immunofluorescence staining (Fig. 4C and D). Knockdown of Orai1 expression with Orai1-specific shRNAs significantly suppressed NFAT4 nuclear accumulation in hypoxic TNBCs (Fig. 4E to G). Consistent with this, DAPT, Notch1 knockdown and SKF96365 also inhibited NFAT4 activation in hypoxic TNBCs (Fig. 4E to G). Together, these results showed that Notch1/Orai1 signaling plays a key role in hypoxia-induced NFAT4 activation in TNBCs.

### 3.5. Orai1 regulates hypoxia-induced cell migration and invasion in TNBCs

To investigate the function of Orai1 in regulating cell motility, we performed the wound healing and migration/invasion assays in hypoxic TNBCs. As shown in Fig. 5A and D, hypoxia enhanced the wound healing ability of MDA-MB 231 and BT549 cells. The migration/invasion assays further demonstrated that hypoxia promoted cell motility in TNBCs (Fig. 5B to F). We also found that hypoxic TNBCs have increased capacity for attachment and detachment (Fig. 5G). More importantly, down-regulation of Orai1/Notch1, DAPT, SKF96365 or FK506, an inhibitor of  $Ca^{2+}$  dependent calcineurin, which dephosphorylates and activates NFAT, markedly reduced cell migration and invasion (Fig. 6A and B). We also found that inhibition of Notch1/Orai1/SOCE/NFAT4 signaling suppressed capacity for hypoxic TNBC attachment and detachment, which is consistent with the migration and invasion findings (Fig. 6C and D). Notably, under hypoxia, inhibition of Notch1/Orai1/SOCE/NFAT4 signaling significantly decreased capacity for motility in hypoxic TNBCs by wound healing assay (Fig. 6E). To investigate the clinical potential of Orai1 in TNBC metastasis, we analyzed TNBC samples from 69 patients (Supplementary Table 1). Orai1 expressions were markedly increased in breast cancer tissues from lymph node metastatic (N1–3) TNBC patients (Supplementary Fig. 2). Together, these results suggested that hypoxia induced cell migration and invasion via Notch1/Orai1/SOCE/NFAT4 pathway.

### 3.6. Orai1 supports hypoxia-induced angiogenesis in TNBCs

Hypoxia contributes tumor progression through the formation of new blood vessels, which is named angiogenesis. The degree of malignancy and patient prognosis is strongly linked to the level of angiogenesis in human tumors including TNBCs [37]. The NFAT signaling is

involved in angiogenesis, but the underlying mechanism is still not well known. To determine whether Notch1/Orai1/SOCE/NFAT4 signaling plays a major role in tumor angiogenesis under hypoxia, we examined the degree of angiogenic induction in HMECs grown in conditioned medium harvested from hypoxic MDA-MB 231 or BT549 cells with different treatment by tube formation assay in vitro. Hypoxia increased angiogenesis in TNBCs (Fig. 7A and B). Inhibition of Orai1 expression markedly reduced the number of branch points (Fig. 7C and D). Consistent with this, pretreatment of TNBCs with DAPT, Notch1 siRNAs, SKF96365, NFAT4 siRNAs or FK506 significantly inhibited hypoxia-induced tube formation (Fig. 7C and D). Together, these results indicated that Notch1/Orai1/SOCE/NFAT4 signaling is essential for hypoxia-induced angiogenic potential of TNBCs.

## 4. Discussion

TNBC is a specifically aggressive type of breast cancer with poor treatment outcomes due to lacking of effective therapeutic targets such as those for luminal and HER2 [1–3]. Invasion of TNBCs is the major reason for unsuccessful surgical therapy [2]. Therefore, understanding the mechanism controlling invasion is necessary for improving survival rates for breast cancer patients. Although Orai1 is now recognized to be an important contributor for breast cancer cell migration, the underlying mechanism and the inducer of this effect remain unclear. To our knowledge, this is the first report to demonstrate that Orai1 expression is elevated in hypoxic TNBCs depending on Notch1 activation. Inhibition of Orai1 suppresses hypoxia-induced migration and invasion in TNBCs. We also provided the evidence that Orai1 enhances aggressive type through NFAT4 signaling. Notch1/Orai1/SOCE/NFAT4 axis supports hypoxia-induced tumor angiogenesis. Therefore, our study highlights the Notch1/Orai1/SOCE/NFAT signaling as being critical for hypoxia-induced migration and invasion in TNBCs (Fig. 8).

Emerging role of the low oxygen environment has been reported to be positively related to human breast cancer aggressiveness and poor prognosis [38]. The role of HIF1 $\alpha$  is well demonstrated in cancer proliferation and invasion [38]. We found that HIF1 $\alpha$  expressions were markedly increased in MDA-MB 231 or BT549 cells under hypoxic conditions compared with those in normoxia. Similarly, Jagged-1 and full-length/cleaved Notch1 expressions were elevated after the hypoxic switch in TNBCs. The Notch target genes HEYL, HES1 and HES5 were also increased. Consistent with these findings, Notch receptors were reported to be differentially expressed in breast cancers depending on the degree of malignancy. The Notch-induced transcriptional targets that contribute to the progression of the aggressive and malignant types in TNBCs are still poorly understood. Orai1 expressions were low in normoxia but markedly enhanced in hypoxic conditions. Pharmacological inhibition or gene knockdown of Notch signaling suppressed hypoxia-induced up-regulation of Orai1 in MDA-MB 231 or BT549 cells, suggesting that Orai1 expression is significantly evaluated in TNBCs exposed to hypoxia in a manner depending on Notch activation. Although Notch signaling is critical for Orai1 up-regulation, it remains to be determined whether the Notch pathway directly or indirectly, through cross talk with other transcription factors, mediates Orai1 transcription [39,40]. Furthermore, hypoxia increased steady-state  $[Ca^{2+}]_i$  and inhibition or knockdown of Orai1 impaired hypoxia-induced up-regulated basal  $[Ca^{2+}]_i$  in TNBCs. It is well known that Orai1 is responsible for SOCE [41,42]. Next, we examined the effect of hypoxia on TG-induced SOCE. We found that Pharmacological inhibition or gene knockdown of Orai1 prevented the increase in TG-induced SOCE under hypoxia conditions in TNBCs. Down-regulation of Orai1 also suppressed the increase in basal  $Ca^{2+}$  influx in hypoxic TNBCs. Therefore, Orai1-mediated SOCE is responsible for the sustained increase in steady-state  $[Ca^{2+}]_i$  in TNBCs exposed to hypoxia. Orai1-mediated SOCE activates NFAT, a family of transcription factors including NFAT4 [35,43]. Opening of store-operated Orai1 channels promotes NFAT4 to migrate from the cytoplasm to the nucleus [44]. Lee

SH et al. found that Orai1 enhances cancer stemness via NFAT4 signaling in oral/oropharyngeal squamous cell carcinoma [45]. There is emerging evidence suggesting that NFAT signaling plays a key role in regulating numbers of target genes involved in the cancer progression [46]. However, the role of NFAT4 proteins in hypoxic TNBC has not been examined. Silencing or inhibition of Orai1 led to suppression of NFAT4 activation in hypoxic TNBCs. Moreover, blocking of Notch signaling also inhibited hypoxia-induced NFAT4 activation in TNBCs. Here, our findings strongly supported the idea that hypoxia induced Notch1/Orai1/SOCE/NFAT4 signaling.

It is well known that hypoxia promotes a motile and invasive phenotype of breast cancer cells, which contributes to therapeutic failure and decreased survival [47–49]. Previous studies showed that Notch signaling mediates hypoxia-induced tumor cell migration and invasion [50].  $Ca^{2+}$  signaling also plays an important role in migration [51]. Therefore, to test whether the induction of aggressive type in TNBCs under hypoxia was dependent on the Notch1/Orai1/SOCE/NFAT4 signaling, we examined the effects of pharmacological inhibition or gene silencing on this signaling. Hypoxia promoted cell migration and invasion in TNBCs and DAPT suppressed these effects of hypoxia. In agreement with the previous findings that inhibition of Orai1 impaired cell migration and invasion, our data showed that the aggressive type of TNBCs induced by hypoxia is dependent on Orai1-mediated SOCE [24]. NFAT signaling plays an essential role in modulating cancer cell motility and invasion [52,53]. Consistent with this notion, we found that inhibition or knockdown of NFAT4, the downstream of Orai1-regulated SOCE, decreased hypoxia-induced migration and invasion in TNBCs, suggesting activation of the calcineurin-NFAT signaling is vital for aggressive progression of TNBC under hypoxia. Moreover, we found Orai1 expressions were significantly increased in N1–3 TNBC patients than that in N0 TNBC patients. Therefore, our findings strongly supported the idea that the Notch1/Orai1/SOCE/NFAT4 signaling is required for up-regulated aggressive type of TNBCs in response to hypoxia. In addition, hypoxia contributes tumor progression through enhanced angiogenesis. A role for Orai1 in regulating vascular endothelial growth factor (VEGF)-activated endothelial tube formation has been suggested [54]. The Orai1-mediated SOCE may contribute to VEGF-dependent angiogenesis. We found that inhibition of the Notch1/Orai1/SOCE/NFAT4 signaling markedly reduced the ability of hypoxic TNBCs to induce endothelial cell tube formation *in vitro*.

Collectively, the results obtained in the present study have demonstrated a novel role for Orai1 in modulating aggressive type of TNBCs in response to hypoxia via the Notch1/Orai1/SOCE/NFAT4 signaling. Our data thus revealed a novel mechanism by which hypoxia controls the angiogenesis and aggression in TNBCs.

## Funding

This work was supported by the National Natural Science Foundation of China (91439131, 81622007 and 81572940); the Natural Science Foundation for Distinguished Young Scholars of Jiangsu Province (BK20140004); the National High Technology Research and Development Program (863 Program) of China (SQ2015AA020948); Jiangsu Province Young Medical Talents (No. QNRC2016153); the Fundamental Research Funds for the Central Universities (JUSRP51704A and JUSRP11747).

## Conflict of interest

We declare that all authors of this manuscript have no conflict of interest to declare.

## Transparency document

The <http://dx.doi.org/10.1016/j.bbadis.2018.01.003> associated with this article can be found, in online version.

## Appendix A. Supplementary data

Supplementary data to this article can be found online at <https://doi.org/10.1016/j.bbadis.2018.01.003>.

## References

- [1] C.E. DeSantis, S.A. Fedewa, A. Goding Sauer, J.L. Kramer, R.A. Smith, A. Jemal, Breast cancer statistics, 2015: convergence of incidence rates between black and white women, *CA Cancer J. Clin.* 66 (2016) 31–42.
- [2] C.A. Hudis, L. Gianni, Triple-negative breast cancer: an unmet medical need, *Oncologist* 16 (Suppl. 1) (2011) 1–11.
- [3] R. Peto, C. Davies, J. Godwin, R. Gray, H.C. Pan, M. Clarke, et al., Comparisons between different polychemotherapy regimens for early breast cancer: meta-analyses of long-term outcome among 100,000 women in 123 randomised trials, *Lancet* 379 (2012) 432–444.
- [4] E.A. Rakha, M.E. El-Sayed, J. Reis-Filho, I.O. Ellis, Patho-biological aspects of basal-like breast cancer, *Breast Cancer Res. Treat.* 113 (2009) 411–422.
- [5] X. Zhu, S. Verma, Targeted therapy in her2-positive metastatic breast cancer: a review of the literature, *Curr. Oncol.* 22 (2015) S19–28.
- [6] J.E. Lang, J.S. Weesler, M.F. Press, D. Tripathy, Molecular markers for breast cancer diagnosis, prognosis and targeted therapy, *J. Surg. Oncol.* 111 (2015) 81–90.
- [7] S.P. Shah, A. Roth, R. Goya, A. Oloumi, G. Ha, Y. Zhao, et al., The clonal and mutational evolution spectrum of primary triple-negative breast cancers, *Nature* 486 (2012) 395–399.
- [8] V.G. Abramson, B.D. Lehmann, T.J. Ballinger, J.A. Pietsenpol, Subtyping of triple-negative breast cancer: implications for therapy, *Cancer* 121 (2015) 8–16.
- [9] M. Reedyk, S. Odorcic, L. Chang, H. Zhang, N. Miller, D.R. McCreedy, et al., High level coexpression of JAG1 and NOTCH1 is observed in human breast cancer and is associated with poor overall survival, *Cancer Res.* 65 (2005) 8530–8537.
- [10] D.R. Robinson, S. Kalyana-Sundaram, Wu YM, S. Shankar, X. Cao, B. Ateeq, et al., Functionally recurrent rearrangements of the MAST kinase and Notch gene families in breast cancer, *Nat. Med.* 17 (2011) 1646–1651.
- [11] V.S. Jamdade, N. Sethi, N.A. Mundhe, P. Kumar, M. Lahkar, N. Sinha, Therapeutic targets of triple-negative breast cancer: a review, *Br. J. Pharmacol.* 172 (2015) 4228–4237.
- [12] S. Artavanis-Tsakonas, M.D. Rand, R.J. Lake, Notch signaling: cell fate control and signal integration in development, *Science* 284 (1999) 770–776.
- [13] C.S. Nowell, F. Radtke, Notch as a tumour suppressor, *Nat. Rev. Cancer* 17 (2017) 145–159.
- [14] J. Speiser, K. Foreman, E. Drinka, C. Godellas, C. Perez, A. Salhadar, et al., Notch1 and Notch4 biomarker expression in triple-negative breast cancer, *Int. J. Surg.* 20 (2012) 139–145.
- [15] P. Toupalikioti, D. Chondronasiou, F. Ziouti, M. Koubanaki, K. Haitoglou, G. Kouvatseas, et al., Expression of Notch receptors in primary breast cancer and correlation with pathological features, *Clin. Exp. Pharmacol.* 2 (2012) 1000109.
- [16] K. Xu, J. Usary, P.C. Kousis, A. Prat, D.Y. Wang, J.R. Adams, et al., Lunatic fringe deficiency cooperates with the Met/Caveolin gene amplicon to induce basal-like breast cancer, *Cancer Cell* 21 (2012) 626–641.
- [17] E.J. Pettit, F.S. Fay, Cytosolic free calcium and the cytoskeleton in the control of leukocyte chemotaxis, *Physiol. Rev.* 78 (1998) 949–967.
- [18] M. Mareel, A. Leroy, Clinical, cellular, and molecular aspects of cancer invasion, *Physiol. Rev.* 83 (2003) 337–376.
- [19] P.W. Marks, F.R. Maxfield, Transient increases in cytosolic free calcium appear to be required for the migration of adherent human neutrophils, *J. Cell Biol.* 110 (1990) 43–52.
- [20] H. Komuro, P. Rakic, Modulation of neuronal migration by NMDA receptors, *Science* 260 (1993) 95–97.
- [21] R.S. Lewis, Store-operated calcium channels: New perspectives on mechanism and function, *Cold Spring Harb. Perspect. Biol.* 3 (2011) (pii:a003970).
- [22] J. Soboloff, B.S. Rothberg, M. Madesh, D.L. Gill, STIM proteins: dynamic calcium signal transducers, *Nat. Rev. Mol. Cell Biol.* 13 (2012) 549–565.
- [23] M. Prakriya, S. Feske, Y. Gwack, S. Srikanth, A. Rao, P.G. Hogan, Orai1 is an essential pore subunit of the CRAC channel, *Nature* 443 (2006) 230–233.
- [24] J. Xia, H. Wang, H. Huang, L. Sun, S. Dong, N. Huang, et al., Elevated Orai1 and STIM1 expressions upregulate MACC1 expression to promote tumor cell proliferation, metabolism, migration, and invasion in human gastric cancer, *Cancer Lett.* 381 (2016) 31–40.
- [25] S. Yang, J.J. Zhang, X.Y. Huang, Orai1 and STIM1 are critical for breast tumor cell migration and metastasis, *Cancer Cell* 15 (2009) 124–134.
- [26] I. Dullloo, B.H. Phang, R. Othman, S.Y. Tan, A. Vijayaraghavan, L.K. Goh, et al., Hypoxia-inducible TAp73 supports tumorigenesis by regulating the angiogenic transcriptome, *Nat. Cell Biol.* 17 (2015) 511–523.
- [27] C.M. Xie, X.Y. Liu, K.W. Sham, J.M. Lai, C.H. Cheng, Silencing of EEF2K (eukaryotic elongation factor-2 kinase) reveals AMPK-ULK1-dependent autophagy in colon cancer cells, *Autophagy* 10 (2014) 1495–1508.
- [28] Y. Wang, Z.C. Li, P. Zhang, E. Poon, C.W. Kong, K.R. Boheler, et al., Nitric oxide-cGMP-PKG pathway acts on Orai1 to inhibit the hypertrophy of human embryonic stem cell-derived cardiomyocytes, *Stem Cells* 33 (2015) 2973–2984.
- [29] P. Zhang, D. He, Z. Chen, Q. Pan, F. Du, X. Zang, et al., Chemotherapy enhances tumor vascularization via Notch signaling-mediated formation of tumor-derived endothelium in breast cancer, *Biochem. Pharmacol.* 118 (2016) 18–30.
- [30] P. Zhang, X. Liu, H. Li, Z. Chen, X. Yao, J. Jin, et al., TRPC5-induced autophagy promotes drug resistance in breast carcinoma via CaMKK $\beta$ /AMPK $\alpha$ /mTOR

- pathway, *Sci. Rep.* 7 (2017) 3158.
- [31] J. Du, X. Ma, B. Shen, Y. Huang, L. Birnbaumer, X. Yao, TRPV4, TRPC1, and TRPP2 assemble to form a flow-sensitive heteromeric channel, *FASEB J.* 28 (2014) 4677–4685.
- [32] Y. Wang, J. Liu, X. Ying, P.C. Lin, B.P. Zhou, Twist-mediated epithelial-mesenchymal transition promotes breast tumor cell invasion via inhibition of Hippo pathway, *Sci. Rep.* 6 (2016) 24606.
- [33] I.G. Rivera, M. Ordoñez, N. Presa, P. Gangoiti, A. Gomez-Larrauri, M. Trueba, et al., Ceramide 1-phosphate regulates cell migration and invasion of human pancreatic cancer cells, *Biochem. Pharmacol.* 102 (2016) 107–119.
- [34] Z. Wang, Y. Li, D. Kong, S. Banerjee, A. Ahmad, A.S. Azmi, et al., Acquisition of epithelial-mesenchymal transition phenotype of gemcitabine-resistant pancreatic cancer cells is linked with activation of the notch signaling pathway, *Cancer Res.* 69 (2009) 2400–2407.
- [35] A.B. Parekh, J.W. Putney Jr., Store-operated calcium channels, *Physiol. Rev.* 85 (2005) 757–810.
- [36] T. Xiao, J.J. Zhu, S. Huang, C. Peng, S. He, J. Du, et al., Phosphorylation of NFAT3 by CDK3 induces cell transformation and promotes tumor growth in skin cancer, *Oncogene* 36 (2017) 2835–2845.
- [37] S.J. Conley, E. Gheordunescu, P. Kakarala, B. Newman, H. Korkaya, A.N. Heath, et al., Antiangiogenic agents increase breast cancer stem cells via the generation of tumor hypoxia, *Proc. Natl. Acad. Sci. U. S. A.* 109 (2012) 2784–2789.
- [38] L. Schito, S. Rey, Hypoxic pathobiology of breast cancer metastasis, *Biochim. Biophys. Acta* 1868 (2017) 239–245.
- [39] M.V. Gustafsson, X. Zheng, T. Pereira, K. Gradin, S. Jin, J. Lundkvist, et al., Hypoxia requires notch signaling to maintain the undifferentiated cell state, *Dev. Cell* 9 (2005) 617–628.
- [40] L.L. Song, Y. Peng, J. Yun, P. Rizzo, V. Chaturvedi, S. Weijzen, et al., Notch-1 associates with IKK $\alpha$  and regulates IKK activity in cervical cancer cells, *Oncogene* 27 (2008) 5833–5844.
- [41] S. Feske, Y. Gwack, M. Prakriya, S. Srikanth, S.H. Puppel, B. Tanasa, et al., A mutation in Orai1 causes immune deficiency by abrogating CRAC channel function, *Nature* 441 (2006) 179–185.
- [42] J.C. Mercer, W.I. Dehaven, J.T. Smyth, B. Wedel, R.R. Boyles, G.S. Bird, et al., Large store-operated calcium selective currents due to co-expression of Orai1 or Orai2 with the intracellular calcium sensor, Stim1, *J. Biol. Chem.* 281 (2006) 24979–24990.
- [43] A.B. Parekh, Functional consequences of activating store operated CRAC channels, *Cell Calcium* 42 (2007) 111–121.
- [44] P. Kar, A.B. Parekh, Distinct spatial Ca<sup>2+</sup> signatures selectively activate different NFAT transcription factor isoforms, *Mol. Cell* 58 (2015) 232–243.
- [45] S.H. Lee, N.K.I. Rigas, C.R. Lee, A. Bang, S. Srikanth, Y. Gwack, Orai1 promotes tumor progression by enhancing cancer stemness via NFAT signaling in oral/oropharyngeal squamous cell carcinoma, *Oncotarget* 7 (2016) 43239–43255.
- [46] M. Mancini, A. Toker, NFAT proteins: emerging roles in cancer progression, *Nat. Rev. Cancer* 9 (2009) 810–820.
- [47] L. Schito, G.L. Semenza, Hypoxia-inducible factors: master regulators of cancer progression, *Trends Cancer* 2 (2016) 758–770.
- [48] J.P. Dales, S. Garcia, S. Meunier-Carpentier, L. Andrac-Meyer, O. Haddad, M.N. Lavaut, et al., Overexpression of hypoxia-inducible factor HIF-1 $\alpha$  predicts early relapse in breast cancer: retrospective study in a series of 745 patients, *Int. J. Cancer* 116 (2005) 734–739.
- [49] S.C. Winter, F.M. Buffa, P. Silva, C. Miller, H.R. Valentine, H. Turley, et al., Relation of a hypoxia metagene derived from head and neck cancer to prognosis of multiple cancers, *Cancer Res.* 67 (2007) 3441–3449.
- [50] C. Sahlgren, M.V. Gustafsson, S. Jin, L. Poellinger, U. Lendahl, Notch signaling mediates hypoxia-induced tumor cell migration and invasion, *Proc. Natl. Acad. Sci. U. S. A.* 105 (2008) 6392–6397.
- [51] J.B. Huang, A.L. Kindzelskii, A.J. Clark, H.R. Petty, Identification of channels promoting calcium spikes and waves in HT1080 tumor cells: their apparent roles in cell motility and invasion, *Cancer Res.* 64 (2004) 2482–2489.
- [52] M. Yoeli-Lerner, G.K. Yiu, I. Rabinovitz, P. Erhardt, S. Jauliac, A. Toker, Akt blocks breast cancer cell motility and invasion through the transcription factor NFAT, *Mol. Cell* 20 (2005) 539–550.
- [53] R.J. Flockhart, J.L. Armstrong, N.J. Reynolds, P.E. Lovat, NFAT signalling is a novel target of oncogenic BRAF in metastatic melanoma, *Br. J. Cancer* 101 (2009) 1448–1455.
- [54] J. Li, R.M. Cubbon, L.A. Wilson, M.S. Amer, L. McKeown, B. Hou, et al., Orai1 and CRAC channel dependence of VEGF-activated Ca<sup>2+</sup> entry and endothelial tube formation, *Circ. Res.* 108 (2011) 1190–1198.